Glycerolipid Composition and Advanced Physicochemical Considerations of Sacha Inchi Oil toward Cosmetic Products Formulation

Diana Penagos-Calvete [1]**, Valeria Duque** [1]**, Claudia Marimon** [1]**, Diana M. Parra** [2]**, Sandra K. Restrepo-Arango** [2]**, Oliver Scherf-Clavel** [3]**, Ulrike Holzgrabe** [3]**, Guillermo Montoya** [2,*]** and Constain H. Salamanca** [1,2,*]

[1] Maestría en Formulación de Productos Químicos y Derivados, Facultad de Ciencias Naturales, Universidad Icesi, Calle 18 No. 122-135, Cali 76003, Colombia; dpenagos@icesi.edu.co (D.P.-C.); valeduke9@hotmail.com (V.D.); claudiapmj@gmail.com (C.M.)

[2] Departamento de Ciencias Farmacéuticas, Facultad de Ciencias Naturales, Universidad Icesi, Cali 76003, Colombia; dianaparra-2006@hotmail.com (D.M.P.); karirestrepo21@gmail.com (S.K.R.-A.)

[3] Institute for Pharmacy and Food Chemistry, University of Würzburg, 97074 Würzburg, Germany; oliver.scherf-clavel@uni-wuerzburg.de (O.S.-C.); ulrike.holzgrabe@uni-wuerzburg.de (U.H.)

[*] Correspondence: glmontoya@icesi.edu.co (G.M.); chsalamanca@icesi.edu.co (C.H.S.)

check for updates

Abstract: Sacha inchi oil is a premier raw material with highly nutritional and functional features for the foodstuff, pharmaceutical, beauty, and personal care industries. One of the most important facts about this oil is the huge chemical content of unsaturated and polyunsaturated fatty acids. However, the current available information on the characterization of the triglyceride composition and the advance physicochemical parameters relevant to emulsion development is limited. Therefore, this research focused on providing a detailed description of the lipid composition using high-resolution tandem mass spectrometry and thorough physicochemical characterization to find the value of the required hydrophilic–lipophilic balance (HLB). For this, a study in the interfacial tension was evaluated, followed by the assessment of different parameters such as creaming index, droplet size, viscosity, zeta potential, pH, and electrical conductivity for a series emulsified at thermal stress condition. The results show that fatty acids are arranged into glycerolipids and the required HLB to achieve the maximum physical stability is around 8.

Keywords: sacha inchi oil; unsaturated fatty acids; triacylglycerides; high-resolution tandem mass spectrometry; emulsions oil-in-water; required hydrophilic–lipophilic balance

1. Introduction

Glycerolipids are the most important source of energy storage in higher eukaryotes and almost all plant oils are derived from seeds or seed mesocarp-like tissues. The consumption of edible vegetal oil is expected to double over the coming decades and, more importantly, oils performing a double role as food ingredient, and exotic-functional constituent in cosmetic formulations. There is an increasing interest in sacha inchi oil (SIO), and its industrialization has apparently supplied the market needs, and new and improved methodologies are being developed to better extract yields and preserve the highest nutritional capacity [1]. *Plukenetia volubilis* L. production has expanded throughout the Andean region, and some researchers are interested in finding more *Plukenetia* species which can be more robust and produce bigger seeds [2]. At the same time, this crop plays a crucial role in the social conflict in Colombia, where it has been used as a voluntary crop substitution for illegal crops, which have been forcefully eradicated.

The conditions of the Andean Amazon expanse are shared between Brazil, Peru, Ecuador, and Colombia, and the Sacha inchi crop is rapidly growing due to these similar soil conditions—specifically pluviosity and light cycles. Sacha inchi production in Colombia is carried out in the states of Putumayo, Cauca, Nariño, and Caquetá, but it is also grown elsewhere due to government initiatives and constitutes one of the new and prominent agricultural products.

Regarding its nutritional properties, SIO is tremendously high in polyunsaturated fatty acids such as alpha linoleic acid (18:3) and linoleic acid (18:2), both constituting between 80 and 85% of the fatty acid content. SIO also contains other unsaturated fatty acids, such as oleic acid (18:1), and even saturated ones like palmitic acid (16:0) and stearic acid (18:0) [3]. This premier oil may have unique nutritional properties compared to other vegetal oils, and therefore, it has been projected as a new leading ingredient for advanced formulations in the cosmetics, pharmaceutical, and food industries. Additionally, its glycerolipid content has also been studied in order to understand its physical, chemical, and functional properties [4].

Regarding the foodstuff industry, SIO could be used as a nutritional alternative equivalent to other types of vegetables oils but with higher nutritional and commercial values. SIO can be used combined with olive oil [5], coconut oil [6], argan oil [7], and avocado oil [8]. For emulsify products development, containing active pharmacological ingredients prone to oxidation, the SIO would be incorporated providing an extra protective effect [9]. On the other hand, in the beauty and personal care industry, this oil provides additional types of cosmetic properties. For instance, the SIO could be employed as a "natural raw material" [10–12], as an "antioxidant ingredient" [13] or, due to its origin, as an "exotic oil" [12].

A handful of studies have reported the chemical composition of SIO [3,14,15], but only a few of them have worked with the physicochemical characterization throughout heterodisperse formulations [16–20]. For this reason, this research has focused on exploring two specific aspects of SIO, corresponding to (i) the detailed characterization of glycerolipids composition, and (ii) the determination of the required hydrophilic–lipophilic balance value (HLB) [21,22]. The HLB value is an important physicochemical parameter commonly used in the development of oil-in-water type emulsions.

2. Materials and Methods

2.1. Sacha Inchi Oil Purchasing

The Sacha inchi (*Plukenetia volubilis* L.) oil is commercially obtained from a small agricultural cooperative located in the Municipality of Santander de Quilichao, (Cauca-Colombia). The industrial extraction process comprises mechanical seed pressing (cold pressing) and correct storage conditioning, which preserves oil oxidation until commercialization. The company provided twenty liters of extra virgin oil for the experimental work.

2.2. Chemical and Reagents

The hypergrade methanol, acetonitrile, and acetone for LC-MS were purchased from Sigma-Aldrich (St Louis, Missouri, USA). Ingredients used in emulsified formulations were steareth 2 (Brij™ S2, HLB = 4.9, melting point = 42 °C–46 °C), steareth 20 (Brij™ S20, HLB = 15.3, melting point = 56 °C–60 °C), glyceryl stearate (Cithrol™ GMS, HLB = 3.8, melting point = 57 °C–60 °C) and polyoxyl 40 stearate (Myrj™ S40, HLB = 17.5, melting point = 44 °C–47 °C), sorbitan oleate (Span™ 80, HLB = 4.3, melting point = 10 °C–12 °C) and polysorbate 80 (Tween™ 80, HLB = 15, melting point = −21 °C) purchased at CRODA (Snaith, UK). Methylparaben and propylparaben were acquired from Sigma-Aldrich (St. Louis, MO, USA). Ultrapure water for chromatographic purposes was obtained from an Arium® pro-VF (Sartorius Stedim) with a resistivity of 15MΩ. cm (at 25 °C).

2.3. Physicochemical Quality Control and Fatty Acid Methyl Ester Profiles of SIO

The physicochemical characterization and analysis of the fatty acid methyl ester profiles of SIO were carried out according to the official methods of the American oil chemists´ society (AOCS) [23] and United Stated pharmacopoeia (USP) [24]. Analysis of the refractive index, saponification value, peroxide index, iodine value, and acid index were carried out according to guidelines AOCS Cc 7-25, AOCS Cd 3-25, AOCS Cd 8-53, AOCS Cd 1c-85, and USP 40 <401>, respectively. At the same time, determination of the fatty acid methyl ester profiles was carried out according to guideline AOCS Ce 1-62. Concerning refractive index, a refractometer Vee Gee C10 was used. The analysis of fatty acid employed a gas chromatograph (Hewlett Packard HP 5890, Series II, Palo Alto, CA, USA) equipped with a flame ionization detector and a BPX70-ms capillary column (30 m × 0.25 mm × 0.25 μm) composed of 70% cyanopropylpolysilphenylene-siloxane. The initial temperature was 150 °C/min, which increased by 5 °C/min up to 240 °C. The injector temperature was 240 °C and the detector temperature was 280 °C, with a split ratio of 1:30. The carrier gas used was He at 1 mL/min, at a pressure of 11 psi.

2.4. Chromatographic and Mass Spectrometry Conditions

The UHPLC system consisted of an UltiMate 3000 thermo-scientific, equipped with a quaternary pump, degasser, and preheater modules. For the chromatographic method, a Develosil 3 μm RP-Aqueous C30 150 × 2 mm, 140 Å pore size column was used in a 105 min run. The mobile phases consisted of acetonitrile/water (80/20 v/v) as eluent A, and methanol/acetone (60/40 v/v) as eluent B using a gradient program as follows: 0 min 70% of A; 10 min 60% A; 15 min 50% A; 20 min 45% A, 30 min 40% A; 45 min 35% A; 55 min 30% A; 65 min 20% A; 70 min 10% A; 85 min 5% A; 90 min 1% A, 95 min 1%A; 100 min 70% A, 105 min 70% A. Flow rate was established at 0.4 mL min^{-1}. The data analysis was carried out using MestRec Nova 11.0. The chromatographic system was coupled to a Q-Exactive hybrid quadrupole-Orbitrap mass spectrometer, using atmospheric pressure chemical ionization ion source in positive mode. The mass spectrometer conditions were a discharge voltage of 2.48 kV, a corona current of 3.50 μA, a capillary temperature of 270 °C, and a vaporizer temperature of 360 °C. Sample preparation for UHPLC-MS analysis was carried out by diluting the sacha inchi oil in the mobile phase B (methanol/acetone 60/40 v/v), to a concentration close to 10 μg/mL.

2.5. Determination of the Required Hydrophilic–Lipophilic Balance Value

Determination of the required HLB value for the SIO was carried out evaluating several methodologies corresponding to interfacial tension, creaming index, drop size, viscosity, zeta potential, pH, and conductivity measurements. For this, several heterodisperse formulations were prepared using SIO, ultrapure water, preservatives (methylparaben and propylparaben), and binary mixtures of different type of surfactants at 2% w/w, which were combined in different proportions to provide HLB values of blend (HLB^B) of 6, 8, 10, and 12 obtained with different mixtures of surfactants (system 1: steareth 2 and steareth 20, system 2: glyceryl stearate and polyoxyl 40 stearate, system 3: Sorbitan oleate and Polysorbate 80). The complete formulations are shown in Supplementary Materials. Each emulsified system was prepared in triplicate.

The values of the HLB surfactants blend were determined according to:

$$HLB^B = HLB_a \times \% \left(S_a \right) + HLB_b \times \% \left(S_b \right) \tag{1}$$

where HLB^B is the value of the binary surfactant blend, and HLB$_a$ and HLB$_b$ are the values of HLB of the respective surfactants used according to the technical sheets. % (S$_a$) and % (S$_b$) is the amount of surfactant mixed considering a base of 100% w/w, with respect to such binary blend.

2.5.1. Emulsion Preparation Method

The emulsions were prepared in several stages according to the formulation shown in support material file. First, the SIO and ultrapure water were heated to 60 °C and 62 °C, respectively. Once the phase temperature was reached, the preservatives were added to the ultrapure water (aqueous phase), while the respective binary surfactant blends (steareth 2-steareth 20, glyceryl stearate-polyoxyl 40 stearate, and poysorbate 80-sorbitan oleate) were added into SIO (oily phase). Afterward, the oily phase was poured into the aqueous phase, using an Ultra-Turrax at 5000 rpm for 10 min. Subsequently, the system was cooled to room temperature, so each emulsified system was ready for further physicochemical characterization studies and thermal stability assays.

2.5.2. Interfacial Tension Measurements

The interfacial tension given between a droplet of SIO immersed in ultrapure water was determined using the pendant drop method [25]. For this, we employed the optical contact angle measuring and contour analysis systems OCA15EC from Dataphysics (Software SCA22 version 4.5.14), coupled with a needle SNP 165/119. Furthermore, this experiment was carried out in the absence and presence of surfactants, where polysorbate 80 was solubilized in ultrapure water, while sorbitan oleate was solubilized in SIO. Each measurement was performed in triplicate at approximately 22 ± 1 °C and $60\% \pm 5\%$ relative humidity.

2.5.3. Creaming Index Determination

In this case, the freshly made emulsions were filled in Falcon™ 15 mL conical centrifuge tubes (diameter = 1.5 cm) and centrifuged at 3000 rmp (150 RFC) for 4 h in a Wincon 80-2 centrifuge (Changsha, China). Finally, the value of the creaming index (CI) was determined according to:

$$CI = \frac{H_S}{H_E} \times 100 \qquad (2)$$

where H_S is the sediment height and H_E is the sample height before centrifugation.

2.5.4. Droplet Size Analysis

The droplet size distribution of the emulsions was obtained using a Mastersizer 3000 (Malvern Instruments, Worcestershire, UK), equipped with a helium/neon laser at a wavelength of 632.8 nm. Previously, ~0.6 g of the emulsion was diluted with 10 mL of ultrapure water at 25 ± 2 °C and stirred at 400 rpm. The appropriate amount sample was determined, when an obscurance level between 2% and 8% was reached in the equipment. Drop size data were expressed as $D_{[4,3]}$ [26–28] and all the measurements were conducted in triplicate.

2.5.5. Viscosity Measurement

Viscosity was measured using a viscometer (micro-visc, RheoSense Inc., San Ramon, CA, USA), applying different shear stress (see support material file). All measurements were performed in triplicate.

2.5.6. Zeta Potential, pH, and Electrical Conductivity Measurements

Zeta potential measurements were carried out using a Zetasizer nano ZSP (Malvern Instruments, Worcestershire, UK) at 25 ± 2 °C temperature, with equilibration times of 120 s in a DTS 1070 capillary cell. For these experiments, the attenuator position and intensity were set automatically. To prepare the sample, ~130 mg of the emulsified system was diluted in 20 mL of ultrapure water and stirred manually. From this, a 50 μL aliquot was taken and diluted with 1 mL of ultrapure water before each zeta potential measurement. On the other hand, the electrical conductivity and pH of the emulsions was determined

using a CR-30 conductivity meter and a Starter-2100 pH meter, respectively. All measurements were carried out in triplicate.

*2.6. Thermal Stability Assay of Sacha Inchi Emulsion*

Once the required HLB value of SIO was found, several oil-in-water emulsions were manufactured in triplicate according to the formulation shown in Supplementary Materials, and the method is described in Section 2.5.1. Each emulsion was placed in Falcon™ 15mL conical centrifuge tubes, which were subsequently left under two temperature conditions (40 ± 2 °C and 4.0 ± 0.5 °C). For this, each thermal condition was varied every week, starting at 40 °C in the first week, then at 4 °C and so on until reaching the last week. The stability parameters evaluated were CI, droplet size, viscosity, zeta potential, pH, and electrical conductivity, which were measured under the same conditions previously described in the section about determining the required HLB.

3. Results and Discussion

3.1. Structural Analysis of Glycerolipids By Mass Spectrometry

Previous reports have focused attention on the fatty acid compositional analysis of SIO [3,4]. They assigned them with the number of carbons followed by the number of double bonds. Linolenic acid, for instance, has three double bonds (Δ9, 12, 15) and is designated as 18:3. Interestingly, the total pattern of glycerolipids in this previous report turns out to be quite similar to our outcomes. We additionally included analysis under high-resolution and tandem mass measurements of the molecular weight and deduced the fatty acid composition using two abundant fragmentations, a neutral loss of each fatty acid, and a specific acyl chain loss that supports the fatty acid composition. These two types of fragmentation paths are explained in Figure 1A–C. β-cleavage is favored and generates a neutral loss of a fatty acid and the formation of a dioxolane linked to the acyl group [29]. The size of the acyl chain depends on the type of fatty acid bonded. The ionization and fragmentation for glycerolipids are favored in atmospheric pressure chemical ionization (APCI) rather than Electrospray ionization (ESI), which give less informative fragments due their neutrality conditions. In order to obtain more structural information by fragmentation, a more energetic mechanism is reached by APCI [30,31]. A MS_2 tandem mass analysis was carried out and the information at the higher collision energy of each compound is reported in Supplementary Materials.

The acyl chains lost were 184, 206, 208, 210, and 212 corresponding to 256 (palmitic acid 16:0), 278 (linolenic acid 18:3), 280 (linoleic acid 18:2), 282 (oleic acid 18:1), and 284 (stearic acid 18:0). The errors in ppm of the glycerolipid (tri and diglycerides) were down 2 ppm, and the neutral fatty acid lost error were under 3 ppm except for compound number 7 (maximum error of 6.7 ppm). The acyl chains lost are explained in Figure 1C showing the fragmentation of TAG10 from Table 1. A complete list of di and triacylglyceroid content are summarized in Table 1. The most abundant compounds were TAG13 with a relative abundance of 7% (18:3,18:1,18:3), TAG14 with 14.7% (18:2,18:3,18:2), TAG15 with 19.7% (18:3,18:2,18:3), and TAG16 with 12.1% (18:3,18:3,18:3). Diacylglycerides DAG17, 18, and 19 are present in relative low abundance in SIO, but also this molecule would be related to a TGA hydrolysis. Our results are in accordance with previous reports regarding chemical profile [4].
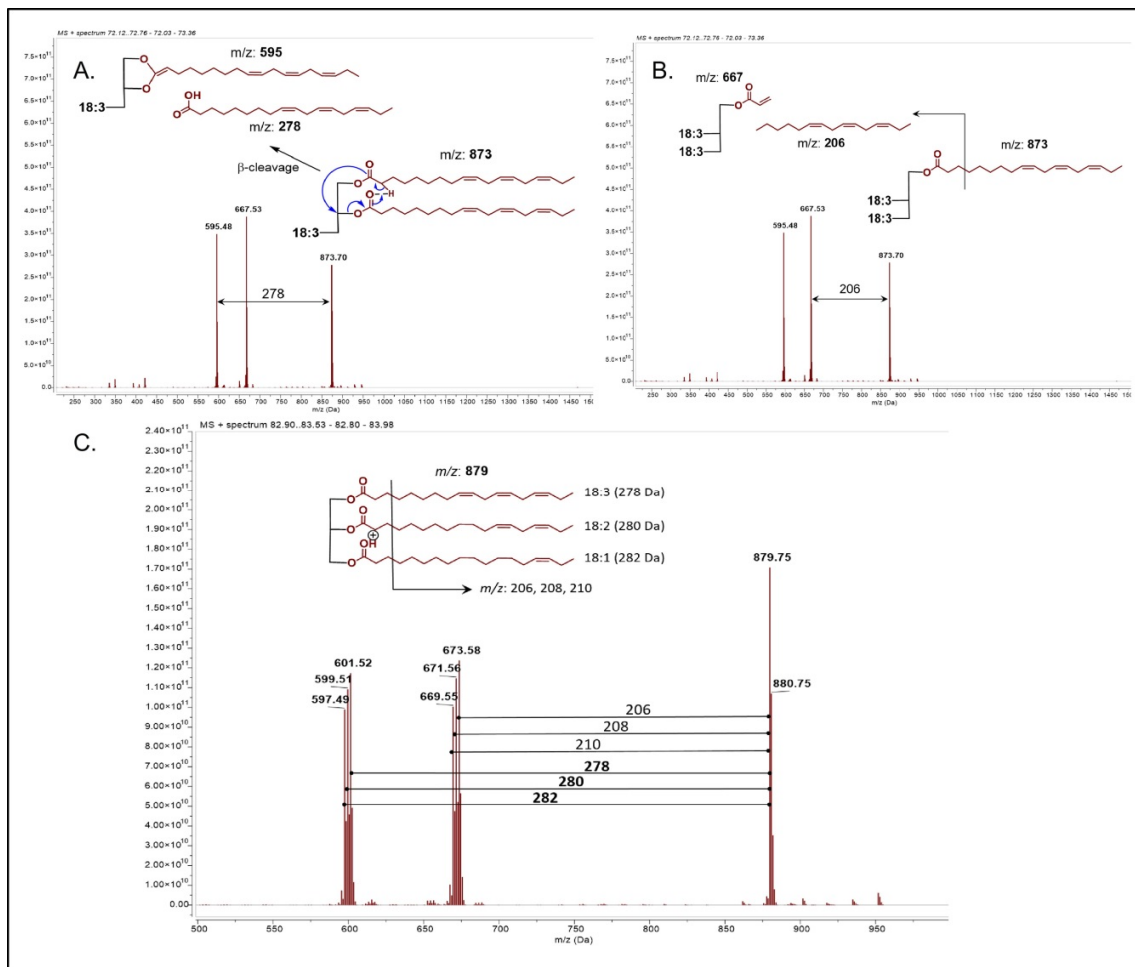
Figure 1. Mass spectrum of TAG 16 (18:3, 18:3, 18:3). (**A**), the fragmentation mechanism explaining the β-cleavage and the neutral loss of one fatty acid. (**B**), the acyl chain loss of 206 corresponding to an 18:3 fatty acid. (**C**), mass spectrum of TAG (18:3, 18:2, 18:1). Different fatty acids linked to glycerol backbone are demonstrated by the three fatty acid losses with their lost acyl chain, respectively.

Table 1. A complete glycerolipid profile under high-resolution mass spectrometry. The reported errors were calculated for each compound, and the neutral fatty acid lost with its error were inferred by subtraction.

		Glycerolipid						Fatty Acid Composition						
		Molecular Formula	Exact Mass	Retention Time	Theorical m/z [M+H]$^+$	Experimental m/z [M+H]$^+$	Error (ppm)	Neutral Fatty Acid Looses	Theorical m/z	Experimental m/z [M+H]$^+$	Error (ppm)	Type of Fatty Acid	Neutral Acyl Moiety Losses	
1	**18:0,18:2,18:2**	$C_{57}H_{102}O_6$	882.76764	98.08	883.77492	883.77509	−0.192	603.53524	280.24023	280.23985	1.356	Linoleic acid (18:2)	675.58824	208.1869
								599.50413	284.27153	284.27096	2.005	Stearic acid (18:0)	671.55205	212.2230
2	**18:2,18:1,16:0**	$C_{55}H_{100}O_6$	856.75199	96.41	857.75927	857.75949	−0.256	601.51960	256.24023	256.23989	1.327	Palmitic acid (16:0)	673.69391	184.0656
								577.51952	280.24023	280.23997	0.928	Linoleic acid (18:2)	649.61682	208.1427
								575.50431	282.25588	282.25518	2.480	Oleic acid (18:1)	647.61991	210.1396
3	**18:1,18:2,18:1**	$C_{57}H_{102}O_6$	882.76764	95.17	883.77492	883.77524	−0.362	601.52011	282.25588	282.25513	2.657	Oleic acid (18:1)	673.58455	210.1907
								603.53434	280.24023	280.24090	−2.391	Linoleic acid (18:2)	675.64272	208.1325
4	**18:0,18:2,18:3**	$C_{57}H_{100}O_6$	880.75199	94.22	881.75927	881.75921	0.068	603.53497	278.22458	278.22424	1.222	Linolenic acid (18:3)	675.59253	206.1667
								597.48834	284.27153	284.27087	2.322	Stearic acid (18:0)	669.54589	212.2133
								601.51945	280.24023	280.23976	1.677	Linoleic acid (18:2)	673.59881	208.1604
5	**16:0,18:1,18:3**	$C_{55}H_{98}O_6$	854.73634	92.82	855.74362	855.74437	−0.876	599.50428	256.24023	256.24009	0.546	Palmitic acid (16:0)	671.56189	184.1825
								577.52001	278.22458	278.22436	0.791	Linolenic acid (18:3)	649.57751	206.1669
								573.48895	282.25588	282.25542	1.630	Oleic acid (18:1)	645.54626	210.1981
6	**18:2,18:2,16:0**	$C_{55}H_{98}O_6$	854.73634	92.12	855.74362	855.74450	−1.028	599.50436	256.24023	256.24014	0.351	Palmitic acid (16:0)	671.56188	184.1826
								575.50448	280.24023	280.24002	0.749	Linoleic acid (18:2)	647.56189	208.1826
7	**18:2,18:1,18:2**	$C_{57}H_{100}O_6$	880.75199	90.67	881.75927	881.75821	1.202	601.51959	280.24023	280.23862	5.745	Linoleic acid (18:2)	673.57718	208.1810
								599.50423	282.25588	282.25398	6.731	Oleic acid (18:1)	671.56171	210.1965
8	**18:3,18:0,18:3**	$C_{57}H_{98}O_6$	878.73634	90.44	879.74362	879.74446	−0.955	601.51975	278.22458	278.22471	−0.467	Linolenic acid (18:3)	673.57741	206.1671
								595.47226	284.27153	284.27220	−2.357	Stearic acid (18:0)	671.56184	208.1826
9	**16:0,18:2,18:3**	$C_{55}H_{96}O_6$	852.72069	88.06	853.72797	853.72858	−0.715	597.48851	256.24023	256.24007	0.624	Palmitic acid (16:0)	669.54608	184.1825
								575.50425	278.22458	278.22433	0.899	Linolenic acid (18:3)	647.56181	206.1668
								573.48877	280.24023	280.23981	1.499	Linoleic acid (18:2)	645.54617	208.1824
10	**18:2,18:1,18:3**	$C_{57}H_{98}O_6$	878.73634	86.74	879.74362	879.74414	−0.591	601.51880	278.22458	278.22534	−2.732	Linolenic acid (18:3)	673.57617	206.1680
								599.50413	280.24023	280.24001	0.785	Linoleic acid (18:2)	671.56159	208.1826
								597.48862	282.25588	282.25552	1.275	Oleic acid (18:1)	669.54603	210.1981
11	**18:2,18:2,18:2**	$C_{57}H_{98}O_6$	878.73634	85.92	879.74362	879.74414	−0.591	599.50413	280.24023	280.24001	0.785	Linoleic acid (18:2)	671.56159	208.1826
12	**16:0,18:3,18:3**	$C_{55}H_{94}O_6$	850.70504	84.33	851.71232	851.71304	−0.845	595.47294	256.24023	256.24010	0.507	Palmitic acid (16:0)	667.53063	184.1824
								573.48877	278.22458	278.22427	1.114	Linolenic acid (18:3)	645.54620	206.1668
13	**18:3,18:1,18:3**	$C_{57}H_{96}O_6$	876.72069	82.06	877.72797	877.72885	−1.003	599.50434	278.22458	278.22451	0.252	Linolenic acid (18:3)	671.56181	206.1670
								595.47321	282.25588	282.25564	0.850	Oleic acid (18:1)	667.53078	210.1981
14	**18:2,18:3,18:2**	$C_{57}H_{96}O_6$	876.72069	81.78	877.72797	877.72856	−0.672	599.50412	278.2246	278.2244	0.503	Linolenic acid (18:3)	671.56144	206.1671
								597.48857	280.2402	280.2400	0.856	Linoleic acid (18:2)	669.54599	208.1826
15	**18:3,18:2,18:3**	$C_{57}H_{94}O_6$	874.70504	78.77	875.71232	875.71305	−0.834	597.48864	278.2246	278.2244	0.611	Linolenic acid (18:3)	669.54608	206.1670
								595.47313	280.2402	280.2399	1.106	Linoleic acid (18:2)	667.53071	208.1823
16	**18:3,18:3,18:3**	$C_{57}H_{92}O_6$	872.68939	75.86	873.69667	873.69751	−0.961	595.47306	278.2246	278.2245	0.467	Linolenic acid (18:3)	667.53057	206.1669
17	**18:2 18:2**	$C_{39}H_{68}O_5$	616.50668	39.29	617.51395	617.51445	−0.810	337.27418	280.2402	280.2403	−0.143	Linoleic acid (18:2)	-	-
18	**18:3 18:2**	$C_{39}H_{66}O_5$	614.49103	32.89	615.49830	615.49868	−0.617	337.27405	278.2246	278.2246	−0.180	Linolenic acid (18:3)	-	-
								335.25850	280.2402	280.2402	0.000	Linoleic acid (18:2)	-	-
19	**18:3 18:3**	$C_{39}H_{64}O_5$	612.47538	27.54	613.48265	613.48300	−0.571	335.25839	278.2246	278.2246	−0.108	Linolenic acid (18:3)	-	-

3.2. Physicochemical Quality Control and Lipid Composition Profile of SIO

The fatty acid composition in vegetable oils can change due to several reasons, such as plant phenotypic variety, plant growing conditions, type of crop nutrients, conditions of oil extraction, etc. Hence, it is practically mandatory to determine the initial physicochemical features of the sacha inchi oil. The results of the physicochemical characterization and fatty acid profile of SIO are summarized in Table 2.

Table 2. Results of physicochemical quality control and the composition of fatty acid methyl ester profiles of Sacha inchi oil.

Physicochemical Parameter		Value
Refractive index		1.4810
Saponification value (mg KOH/g)		251.72
Peroxide index (meq O/kg)		14.77
Iodine value (g I_2/100g)		195.05
Acid index (% oleic acid)		1.31
Profile of lipid composition (% w/w)		
Common name/shorthand	**IUPAC Name**	**Value**
Myristc acid/C14:0	Tetradecanoic acid	0.02
Palmitic acid/C16:0	Hexadecanoic acid	3.89
Palmitoleic acid/C16:1(n-7)	(Z)-hexadec-9-enoic acid	0.06
Heptadecanoic acid/C17:0	Heptadecanoic acid	0.07
Heptadecanoic acid/C17:1(n-7)	(Z)-heptadec-9-enoic acid	0.03
Stearic acid/C18:0	Octadecanoic acid	2.80
Oleic acid/C18:1(n-9)	(Z)-octadec-9-enoic acid	9.34
Linoleic acid (LA)/C18:2(n-6)	(9Z,12Z)-octadeca-9,12-dienoic acid	35.01
Linolenic acid (ALA)/C18:3(n-3)	(9Z,12Z,15Z)-octadeca-9,12,15-trienoic acid	48.39
Arachidic acid/C20:0	Icosanoic acid	0.07
Gadoleic acid/C20:1(n-9)	(Z)-icos-9-enoic acid	0.30
Behenic acid/C22:0	Docosanoic acid	0.02

The results of refractive index, saponification value, peroxide value, iodine value, acidity index, amount of saturated fat (6.87%), amount of monounsaturated fat (9.73%), and amount of polyunsaturated fat (83.40%), as well as the composition of omega-3 (48.39%), omega-6 (35.01%), and omega-9 (9.64%) were very similar to the previously reported values for this oil [15]. However, it is important to note that the value obtained from the acid number (% oleic acid) is greater than 1%, and with this, such raw material does not correspond to an extra virgin oil.

3.3. Determination of the Required HLB for SIO

3.3.1. Interfacial Tension Measurements

The interfacial tension ($\gamma_{o\text{-}w}$) generated in a heterogeneous system conformed by oil and water is due to several unfavorable thermodynamic phenomena, such as the incapability of the dispersing phase (water) to disintegrate the oil and generate a dispersed phase, and the incapability of the dispersing phase to generate the well-known "solvation box" [32]. In addition to the enthalpic factors just mentioned, there are also other phenomena that lead to the formation of the heterogeneous system and that correspond to the entropic factor. This factor is related to the decrease in the thermal-random motion of the water molecules, which are immediately joined to the layer of the oily phase. Such an entropic factor is the main reason for destabilization in heterodisperse systems (emulsions), because this leads to a series of dynamic events that end with the break of the system (phase separation), creating a tiny contact area known as an interface flat [33,34]. Therefore, in this assay, polysorbate 80 and sorbitan 80 surfactants were selected due to several reasons. (i) They allow obtaining different

values of surfactant blend (HLB^B). (ii) The lengths of their alkyl chains coincide with the lengths of the hydrocarbon chains of the fatty acids in SIO, favoring a better interaction between oil phase and the surfactants. (iii) At room temperature they are liquid, easing the incorporation and solubilization in the respective phases of the emulsion. Regarding the measurements of interfacial tension formed between SIO and ultrapure water, it was found that $\gamma_{o\text{-}w}$ value was 40.7 ± 3.0 mN/m. However, this value decreased with the incorporation of the surfactants in the system, where the blend of surfactants with HLB^B values of 8 and 10 led to reduction in $\gamma_{o\text{-}w}$ value until 4.4 ± 1.1 mN/m and 6.9 ± 0.6 mN/m, respectively, as shown in Figure 2. In this way, the change in $\gamma_{o\text{-}w}$ suggests that the required HLB^B value to achieve the maximum stabilization of SIO is around eight.
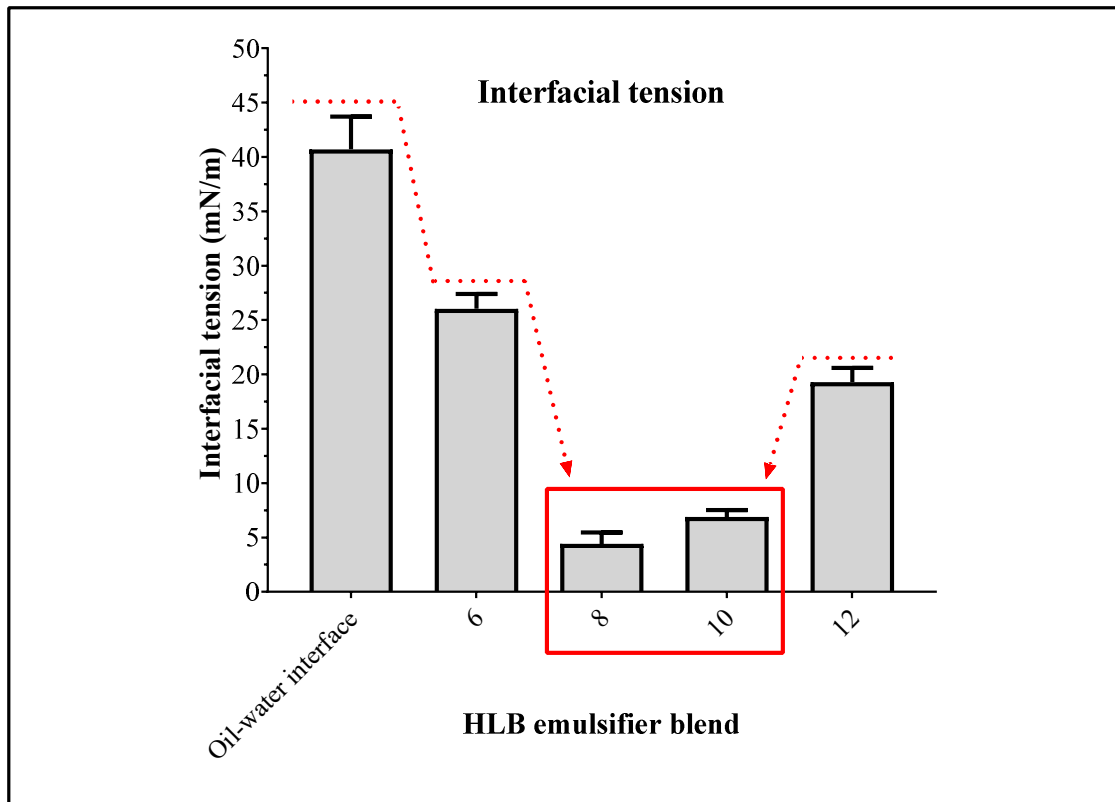
Figure 2. Change of interfacial tension formed between sacha inchi oil and ultra-pure water at different values of HLB surfactants blend.

On the other hand, the results corresponding to physicochemical characterization of the emulsion made up with SIO are depicted in Figure 3.
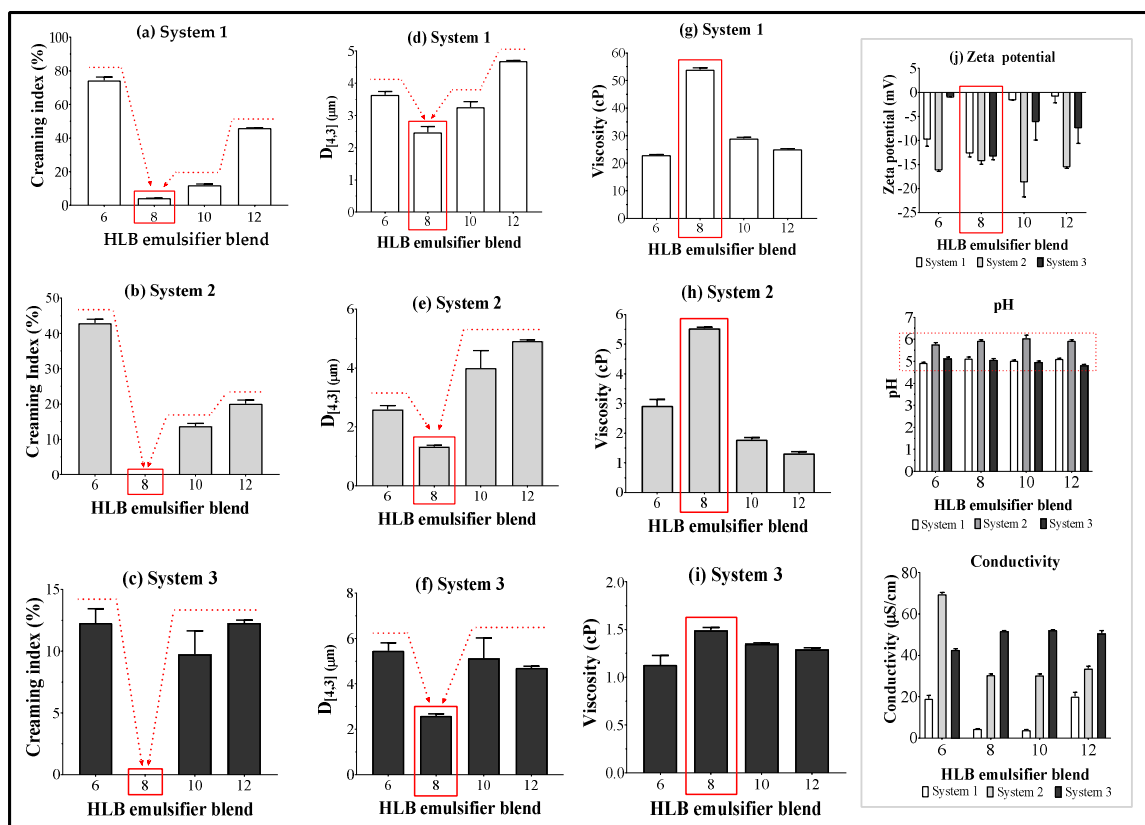
Figure 3. Physicochemical characterization of oil-in-water emulsions elaborated with SIO at different values of HLB surfactants blend, where system 1 corresponds to steareth 2 + steareth 20, system 2 corresponds to glyceryl stearate + polyoxyl 40 stearate and system 3 corresponds to sorbitan oleate + polysorbate 80.

3.3.2. Creaming Index and Droplet Size

The first aspect to highlight in this study is the low amount of surfactant blend used in the emulsified formulations (2% w/w), and therefore, it is possible to guarantee that the stabilization effect in the heterodisperse systems is provided exclusively by the capability of the surfactants to reduce the interface tension and not due to other effects, like micellar stabilization or rheological stabilization.

With respect to the results of CI at zero-time, it was found that surfactant blends with $HLB^B = 8$ always cause the lowest IC (Figure 3a–c), reaching values of 4.3 ± 0.1 for system 1 and 0 for systems 2 and 3. These results are very consistent with those previously obtained in the interfacial tension assays, as well as those found by Kiattiphumi and Ampa [16], who reported that the HLB^B value that leads to the maximum stabilization of oil-in-water emulsions made with SIO was 8.5. However, it should be mentioned that in such a study, they evaluated different conditions than those employed by us, where they used a lower proportion oil (5% w/w), a higher concentration of surfactant blend (5% w/w), and a thickening agent as a co-stabilizer.

In regard to the droplet size data (Figure 3d–f), it was found that these results also show a similar behavior to that described in the interfacial tension and CI assays, where the lowest droplet size values (between 1.3 μm and 2.6 μm) were reached at $HLB^B = 8.0$. Such particle sizes also suggest that the dispersed oil droplets are well stabilized, quite possibly by the formation of a compact layer of surfactants at the interface.

3.3.3. Viscosity Assay

The results of the viscosity assay also agree with those results previously obtained in the studies of interfacial tension, CI, and droplet size, where the maximum viscosity values were achieved

when the HLB^B = 8 (Figure 3g–i). This behavior could be explained, considering the formation of compact oil droplets very well stabilized, which interact in situ, with other stabilized droplets, where the polyethoxylated groups of the hydrophilic surfactants (steareth 20, polyoxyl-40-stearate, and polysorbate 80) form hydrogen bonds that increase the cohesiveness in the system, and thus, the viscosity. On the other hand, the differences observed in viscosity values for the emulsified systems could be explained according to the physicochemical features of the surfactants employed. In the case of system 1, which showed the higher viscosity value (~54.0 Cp) followed by system 2 (~5.5 Cp), the surfactant used are waxes at room temperature, and thus, during the emulsification process and specifically the cooling step, those surfactants solidify, forming interfacial films that are very compact and viscous [35]. On the contrary, system 3 showed the lowest viscosity value (1.5 cp), where the surfactants used are liquid, which form less compact interfacial layers.

3.3.4. Zeta Potential, Ph, and Conductivity

The results of zeta potential (Figure 3j) are very interesting if we consider that all the surfactants used in the study were neutral, and therefore, the zeta potential values should be very close to zero. However, all the zeta potential values obtained were negative. Such behavior can be explained due to the spontaneous formation of a tiny monolayer of hydroxyl ions located in the interface oil-surfactant-water and which come from the autoprotolysis of water [36,37]. Regarding the electrical conductivity values, they can be attributed to the presence of hydronium and hydroxyl ions from the autoprotolysis of water, as well as the ions from the ionization of carbonic acid present in the medium. Although there is not a tendency between the conductivity and the HLB^B values, it can be possible to note that system 1 has the lowest conductivity values (<20 μS/m), while system 3 has the highest conductivity values (>40 μS/m). These results are very consistent, considering that at high viscosity there is low ionic mobility, and thus, system 1 has high viscosity and low conductivity, while system 3 is the opposite. In contrast, the pH characterization of emulsified systems always described slightly acidic values (pH = 5–6). Such a result is attributed to the possible incorporation of CO_2 (gas) into the emulsions during the emulsification process, where such gas is subsequently transformed into carbonic acid.

3.4. Thermal Stability Assay of Sacha Inchi Emulsion

Thermal stress stability studies are very important in the primary stages of formulation or evaluation of prototypes (product pre-formulation), because they provide information in a very short time (1 month) about the possible physical, chemical, and microbiological changes that the system could undergo [38]. For this study, the thermal stability analysis was addressed only to establish the physical changes in the emulsified system, and therefore corroborate if the required HLB values for the SIO found at zero time remained constant or varied. For this, the first parameter analyzed was the CI, which is strongly related to the final stage of physical destabilization for a heterodisperse system (emulsion breaking) [39]. In the case of CI values at time zero for the system 1, it was found that the lowest value of such a parameter (CI = 4.3 ± 0.1) was reached when the emulsions had a HLB^B of eight (Figure 3a). However, with time, these systems start to separate phases after the second week and only the formulations with a HLB^B value of ten remained stable. Hence, the data reported for system 1 corresponds to the emulsion with a value of HLB^B of ten. On the other hand, the emulsions of systems 2 and 3 were stable only at values of HLB^B of eight. In general, physical changes were observed changes regarding CI, droplet size, viscosity, zeta potential, pH, and electrical conductivity for all the emulsified systems from the first week. These changes are shown in Figure 4.
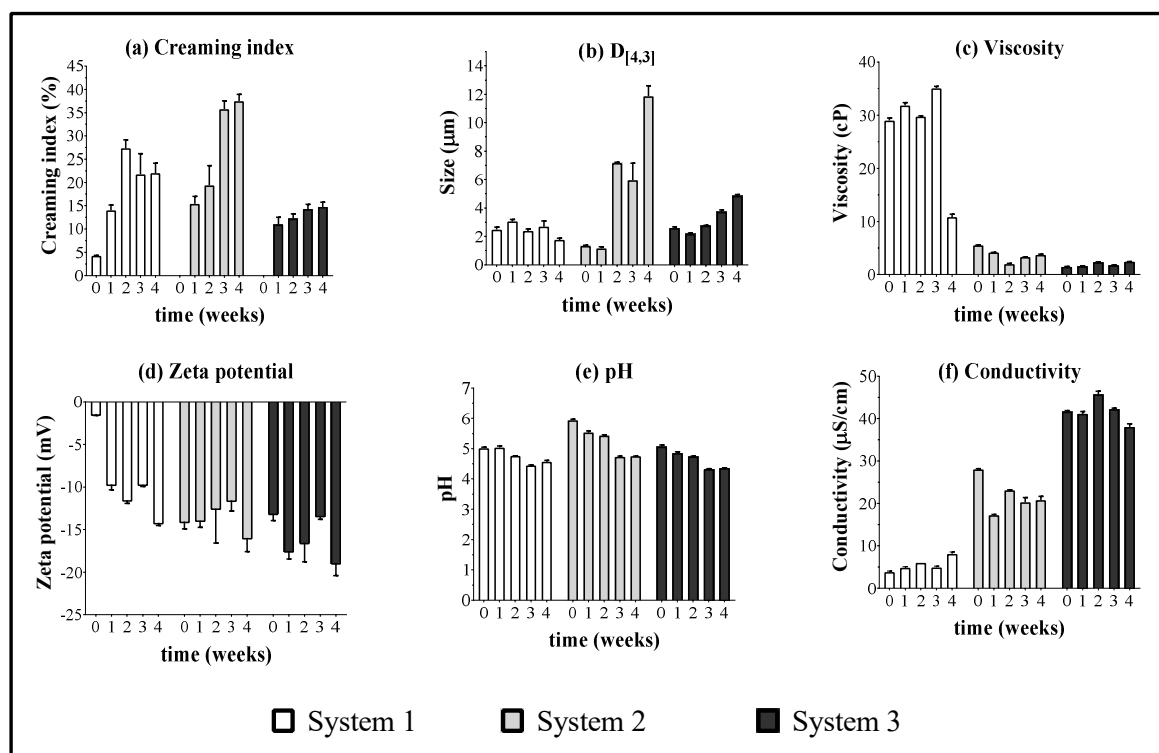
Figure 4. Physicochemical characterization of oil-in-water emulsions to thermal stress conditions. The data of system 1 corresponds to the formulations with a HLBB of ten, whilst the systems 2 and 3 correspond to the formulations with HLBB of eight.

According to system 1, which had steareth 2 and steareth 20 as surfactant blend, it was found that these provided the least capability to stabilize the emulsified formulations of sacha inchi and the results obtained did not depend only on interfacial phenomena (HLB^B), but also on other factors such as rheological stabilization. On the contrary, systems 2 and 3 show a better capability to stabilize the emulsions. In relation to system 2, which had surfactants glyceryl stearate and polyoxyl 40 stearate, we appreciated an appropriate stabilization of the emulsions. However, after the second week, the CI values increased, as well as the droplet size. Regarding system 3, it proved to be the most effective to stabilize the emulsified systems, due to the lower CI values obtained and slight changes in droplet size; even so, this system had the lowest viscosity values. This result can be explained considering that sorbitan 80 and polysorbate 80 surfactants have alkyl chains quite similar to those present in the fatty acids in SIO. Also, such surfactants are easier to incorporate in the respective emulsion phases than the rest of the surfactants evaluated. For the results of zeta potential and conductivity, there were no marked changes with respect to study time. On the other hand, no trend was observed between the pH and the time of the thermal stability assay, where such parameters remained constant between 5 and 6, which is explained by the possible formation of carbonic acid, as described above.

4. Conclusions

The physicochemical characterization of the emulsions prepared with SIO showed values very similar to those previously reported for this oil. Likewise, it was found that the composition of fatty acids, and especially the omega-3 (48.39%), omega-6 (35.01%), and omega-9 (9.64%), also coincides with the previous description given for other sacha inchi oil (*volubilis* variety).

It was also observed that the maximum decrease of the interfacial tension between SIO and ultrapure water was achieved, when the surfactant blend has a value of HLB^B of eight. Equally, it was found that at such HLB^B value, the maximum stabilization of the emulsions is reached. In relation to the different mixtures of surfactants used, the blend of sorbitan 80 and polysorbate 80 proved to be the most

effective to stabilize emulsions elaborated with sacha inchi. The fatty acid composition of SIO displayed a high profile of unsaturated fatty acid, in which 50% of them are arranged in TAG13 (18:3,18:1,18:3), TAG14 (18:2,18:3,18:2), TAG15 (18:3,18:2,18:3), and TAG16 (18:3,18:3,18:3). Diacylglycerides comprise close to 8% of relative abundance in SIO. Due the complexity of analyzed TAG and DAG using conventional techniques, high-resolution mass spectrometry with APCI ion source turns out to be an excellent analytical tool, not only for chemical characterization, but also for quality control during extraction of raw material and monitoring throughout further processing.

On the other hand, the physical–chemical characterization of the oil and emulsions provided a starting point for advance formulation for several industries like cosmetic, pharmaceutical, and foodstuff. Keeping in mind the exceptional nutritional features, this oil will be undeniably converted in the next decades into input for new product formulations. Also, seeing the tremendous impact of illicit crop replacement over the conflict in Colombia, and at the same time bearing in mind its quality, the authors encourage the Colombian government to extend and support the conditions to provide peasants and remote provinces located in the conflict area to establish a new and highly prolific economic chain from the vast and fruitful agriculture that the country has. The most remote regions (Putumayo, Cauca, Nariño, and Caquetá departments) have the greatest and most extraordinary ground conditions for its culture, which makes it a successful and strategical decision.

References

1. Follegatti-Romero, L.A.; Piantino, C.R.; Grimaldi, R.; Cabral, F.A. Supercritical CO_2 extraction of omega-3 rich oil from Sacha inchi (*Plukenetia volubilis* L.) seeds. *J. Supercrit. Fluids* **2009**, *49*, 323–329. [CrossRef]

2. Marris, E. Amazon plant discovery could yield green cash crop. *Nature* **2013**. [CrossRef]

3. Wang, S.; Zhu, F.; Kakuda, Y. Sacha inchi (*Plukenetia volubilis* L.): Nutritional composition, biological activity, and uses. *Food Chem.* **2018**, *265*, 316–328. [CrossRef]

4. Fanali, C.; Dugo, L.; Cacciola, F.; Beccaria, M.; Grasso, S.; Dachà, M.; Dugo, P.; Mondello, L. Chemical characterization of Sacha inchi (*Plukenetia volubilis* L.) oil. *J. Agric. Food Chem.* **2011**, *59*, 13043–13049. [CrossRef]

5. Calabriso, N.; Scoditti, E.; Pellegrino, M.; Carluccio, M.A. Olive oil. In *The Mediterranean Diet: An Evidence-Based Approach*; Academic Press: Cambridge, MA, USA, 2014; ISBN 9780124079427.

6. Bährle-Rapp, M. Coconut oil. In *Springer Lexikon Kosmetik und Körperpflege*; Springer: Berlin/Heidelberg, Germany, 2010.

7. Maleš, Ž.; Mišković, G.; Bojić, M.; Ćurak, I. Argan oil. *Farm. Glas.* **2018**, *74*, 817–824.

8. Duarte, P.F.; Chaves, M.A.; Borges, C.D.; Mendonça, C.R.B. Avocado: Characteristics, health benefits, and uses. *Int. News Fats Oils Relat. Mater.* **2016**, *46*, 747–754. [CrossRef]

9. Gülçin, I.; Elmastaş, M.; Aboul-Enein, H.Y. Antioxidant activity of clove oil—A powerful antioxidant source. *Arab. J. Chem.* **2012**, *5*, 489–499. [CrossRef]

10. Juliano, C.; Magrini, G. Cosmetic functional ingredients from botanical sources for anti-pollution skincare products. *Cosmetics* **2018**, *5*, 19. [CrossRef]

11. Fonseca-Santos, B.; Corrêa, M.A.; Chorilli, M. Sustainability, natural and organic cosmetics: Consumer, products, efficacy, toxicological and regulatory considerations. *Braz. J. Pharm. Sci.* **2015**, *51*, 17–26. [CrossRef]

12. Matić, M.; Puh, B. Consumers' purchase intentions towards natural cosmetics. *Ekon. Vjesn.* **2016**, *29*, 53–64.

13. Moure, A.; Cruz, J.M.; Franco, D.; Domínguez, J.M.; Sineiro, J.; Domínguez, H.; Núñez, M.J.; Parajó, J.C. Natural antioxidants from residual sources. *Food Chem.* **2001**, *72*, 145–171. [CrossRef]

14. Gonzales, G.F.; Gonzales, C.; Villegas, L. Exposure of fatty acids after a single oral administration of sacha inchi (*Plukenetia volubilis* L.) and sunflower oil in human adult subjects. *Toxicol. Mech. Methods* **2014**, *24*, 60–69. [CrossRef]

15. Vicente, J.; de Carvalho, M.G.; Garcia-Rojas, E.E. Fatty acids profile of sacha inchi oil and blends by 1 H NMR and GC-FID. *Food Chem.* **2015**, *181*, 215–221. [CrossRef]

16. Saengsorn, K.; Jimtaisong, A. Determination of hydrophilic–lipophilic balance value and emulsion properties of sacha inchi oil. *Asian Pac. J. Trop. Biomed.* **2017**, *7*, 1092–1096. [CrossRef]

17. Tunkam, P.; Satirapipathkul, C. Preparation of nanoemulsion from sacha inchi oil/water by emulsion phase inversion methods. *Key Eng. Mater.* **2016**, *675*, 57–60. [CrossRef]

18. Silva, K.F.C.E.; da Silva Carvalho, A.G.; Rabelo, R.S.; Hubinger, M.D. Sacha inchi oil encapsulation: Emulsion and alginate beads characterization. *Food Bioprod. Process.* **2019**, *116*, 118–129. [CrossRef]

19. Sanchez-Reinoso, Z.; Gutiérrez, L.F. Effects of the emulsion composition on the physical properties and oxidative stability of sacha inchi (*Plukenetia volubilis* L.) oil microcapsules produced by spray drying. *Food Bioprocess Technol.* **2017**, *10*, 1354–1366. [CrossRef]

20. Vicente, J.; Pereira, L.J.B.; Garcia-Rojas, E.E.; de Souza Cezarino, T.; de Carvalho, M.G.; da Rocha, E.P.; Sá, G.R.; Gamallo, O.D. Microencapsulation of sacha inchi oil using emulsion-based delivery systems. *Food Res. Int.* **2017**, *99*, 612–622. [CrossRef]

21. Fernandes, C.P.; Mascarenhas, M.P.; Zibetti, F.M.; Lima, B.G.; Oliveira, R.P.R.F.; Rocha, L.; Falcão, D.Q. HLB value, an important parameter for the development of essential oil phytopharmaceuticals. *Braz. J. Pharmacogn.* **2013**, *23*, 108–114. [CrossRef]

22. Schmidts, T.; Schlupp, P.; Gross, A.; Dobler, D.; Runkel, F. Required HLB determination of some pharmaceutical oils in submicron emulsions. *J. Dispers. Sci. Technol.* **2012**, *33*, 816–820. [CrossRef]

23. American Oil Chemists' Society. *Official Methods and Recommended Practices of the AOCS*; American Oil Chemists' Society: Champaign, IL, USA, 2017.

24. U.S. Pharmacopoeia. *USP <191> Identification Tests—General*; U.S. Pharmacopoeia: Rockville, MD, USA, 2018.

25. Kahl, H.; Wadewitz, T.; Winkelmann, J. Surface tension of pure liquids and binary liquid mixtures. *J. Chem. Eng. Data* **2003**, *48*, 580–586. [CrossRef]

26. Barth, H.G.; Sun, S.T. Particle size analysis. *Anal. Chem.* **1989**, *61*, 143–152. [CrossRef]

27. Amziane, S.; Collet, F.; Lawrence, M.; Magniont, C.; Picandet, V.; Sonebi, M. Recommendation of the RILEM TC 236-BBM: Characterization testing of hemp shiv to determine the initial water content, water absorption, dry density, particle size distribution and thermal conductivity. *Mater. Struct.* **2017**, *50*. [CrossRef]

28. Picandet, V. Particle size distribution. In *RILEM State-of-the-Art Reports*; Springer: Dordrecht, The Netherlands, 2017.

29. Hsu, F.F.; Turk, J. Electrospray ionization multiple-stage linear ion-trap mass spectrometry for structural elucidation of triacylglycerols: Assignment of fatty acyl groups on the glycerol backbone and location of double bonds. *J. Am. Soc. Mass Spectrom.* **2010**, *21*, 657–669. [CrossRef]

30. Xu, Y.; Brenna, J.T. Atmospheric pressure covalent adduct chemical ionization tandem mass spectrometry for double bond localization in monoene-and diene-containing triacylglycerols. *Anal. Chem.* **2007**, *79*, 2525–2536. [CrossRef]

31. Murphy, R.C.; Leiker, T.J.; Barkley, R.M. Glycerolipid and cholesterol ester analyses in biological samples by mass spectrometry. *Biochim. Biophys. Acta Mol. Cell Biol. Lipids* **2011**, *1811*, 776–783. [CrossRef]

32. Blees, M.H. Foundations of colloid science. *Colloids Surfaces A Physicochem. Eng. Asp.* **2002**, *210*, 125. [CrossRef]

33. Wang, S.; Zhang, Y.; Abidi, N.; Cabrales, L. Wettability and surface free energy of graphene films. *Langmuir* **2009**, *25*, 11078–11081. [CrossRef]

34. Silverstein, T.P. The real reason why oil and water don't mix. *J. Chem. Educ.* **1998**, *75*, 116. [CrossRef]

35. Avranas, A.; Stalidis, G. Interfacial properties and stability of oil-in-water emulsions stabilized with binary mixtures of surfactants. *J. Colloid Interface Sci.* **1991**, *143*, 180–187. [CrossRef]

36. Hunter, R.J. *Zeta Potential in Colloid Science: Principles and Applications*; Academic Press: Cambridge, MA, USA, 2013; ISBN 9781483214085.

37. Wiącek, A.; Chibowski, E. Zeta potential, effective diameter and multimodal size distribution in oil/water emulsion. *Colloids Surfaces A Physicochem. Eng. Asp.* **1999**, *159*, 253–261. [CrossRef]

38. Han, J.; Davis, S.S.; Washington, C. Physical properties and stability of two emulsion formulations of propofol. *Int. J. Pharm.* **2001**, *215*, 207–220. [CrossRef]

39. French, D.J.; Taylor, P.; Fowler, J.; Clegg, P.S. Making and breaking bridges in a Pickering emulsion. *J. Colloid Interface Sci.* **2015**, *441*, 30–38. [CrossRef]